

Impact of stratospheric ozone on paleoclimate reconstruction: Mid-Holocene experiment by using MRI Earth System Model

NODA, Satoshi¹ ; MIZUTA, Ryo² ; DEUSHI, Makoto² ; KODERA, Kunihiko³ ; YOSHIDA, Kohei² ; KITO, Akio⁴ ; MURAKAMI, Shigenori⁵ ; ADACHI, Yukimasa² ; YODEN, Shigeo^{1*}

¹Graduate School of Science, Kyoto University, ²Meteorological Research Institute, ³Solar-Terrestrial Environment Laboratory, Nagoya University, ⁴Graduate School of Life and Environmental Sciences, University of Tsukuba, ⁵Meteorological College

Numerical experiment of mid-Holocene (6000 years before present) is performed by using Meteorological Research Institute Earth System Model (MRI-ESM) to investigate the impact of ozone distribution which is modulated by orbital elements on the tropospheric climate. The result of interactive ozone calculation is compared to those of mid-Holocene and pre-industrial control experiments in CMIP5/PMIP3, in which the ozone distribution was fixed to the value of 1850. Contribution of the chemical processes shows anomaly up to +1.7 K in the Antarctic regions for the annual mean zonal mean temperature at 2 m from the surface. This impact is caused by decrease in the area of sea ice, and the interrelationship in the trend is found to be opposite to that of sea ice and the Antarctic ozone hole as observed in these decades.

Stratospheric warming in the Antarctic spring due to the positive anomaly of ozone causes negative westerly anomaly of the polar night jet by the thermal wind balance, and the annular mode response brings westerly anomaly near the surface. The decrease of the surface westerly weakens the northward component of the Ekman transport in the ocean, suppresses the sea ice transport to lower latitudes, and produces the warming in the polar region.

The importance of chemical feedbacks is supported by a correction of cold bias of SST in the southern hemisphere which is commonly seen in results of CMIP5/PMIP3 models. The comparison between the time variation of the sea ice distribution and that of the stratosphere-troposphere coupling patterns show the importance of coupled chemistry process related to ozone in the reconstruction of mid-Holocene climate.

Keywords: ozone, solar radiation, paleoclimate, earth system model, sea ice

Climatology of the polar thermosphere and ionosphere

FUJIWARA, Hitoshi^{1*} ; MIYOSHI, Yasunobu² ; JIN, Hidekatsu³ ; SHINAGAWA, Hiroyuki³ ;
NOZAWA, Satonori⁴ ; OGAWA, Yasunobu⁵ ; KATAOKA, Ryuhō⁵

¹Faculty of Science and Technology, Seikei University, ²Department of Earth and Planetary Sciences, Faculty of Sciences, Kyushu University, ³National Institute of Information and Communications Technology, ⁴Solar Terrestrial Environment Laboratory, Nagoya University, ⁵National Institute of Polar Research

Recent observations from satellites and ground-based instruments have clarified various phenomena in the polar thermosphere and ionosphere, in particular, the cusp and polar cap region. The CHAMP satellite observations for a decade were the great success to understand the mass density variations in the global thermosphere. However, some basic features and/or climatology of the polar thermosphere and ionosphere seem to be still unknown. For example, amplitudes of the temperature and wind variations during a solar cycle are not exactly known in the local area in and/or in the vicinity of the cusp/polar cap region. In addition, contributions of the lower atmosphere to the temperature and wind variations in the thermosphere seem not to be understood quantitatively in each local area. In order to understand climatology of the polar thermosphere and ionosphere, we have made some observations with the EISCAT radar system and optical instruments in 2011-2015 and performed numerical simulations with a whole atmosphere GCM. The five-year observations of the polar ionosphere with the EISCAT radar system show the large difference between the ionospheres over Longyearbyen and Tromsø; variations of the dayside ion temperature and ion motion at Longyearbyen are larger than those at Tromsø on average during geomagnetically quiet periods. The EISCAT data during the extremely low solar activity 2007-2008 have also clarified the basic state of the ionosphere which would be strongly affected by the lower atmosphere. We will show the recent progress of our understandings of basic features of the polar thermosphere and ionosphere from the observations and GCM simulations.

Keywords: thermosphere, ionosphere, polar region, EISCAT, GCM, simulation

Analysis of occurrence characteristics of sporadic E layers using GAIA

SHINAGAWA, Hiroyuki^{1*} ; MIYOSHI, Yasunobu² ; JIN, Hidekatsu¹ ; FUJIWARA, Hitoshi³

¹NICT, ²Kyushu University, ³Seikei University

Sporadic E (Es) is a high-density ion layer formed in a narrow-altitude region between about 90 km and 120 km. Since Es has significant influences on radio communications and broadcast, it is one of the most important phenomena in space weather forecast. Although it is generally accepted that Es is formed by combination of neutral wind shear and metallic ions originated from meteor ionization in the lower thermosphere and in the upper mesosphere, the mechanisms of formation and variation of Es have not been quantitatively understood. Previous observations have indicated that Es has clear seasonal and local time variations and geographic location dependences. One of the most prominent features of Es is that Es appears most frequently in the mid-latitude east Asian region in the northern hemispheric summer, and in the mid-latitude South American region in the southern hemispheric summer. This phenomenon has been recognized for a long time, but no theoretical explanation has been given until now. Our group has been developing GAIA (Ground-to-topside model of Atmosphere and Ionosphere for Aeronomy), which self-consistently includes the whole atmosphere and the ionosphere with meteorological reanalysis data introduced in the lower atmosphere. Although the resolution of GAIA is still not enough to directly reproduce Es, it is expected that the model can give at least a clue to estimating occurrence conditions of Es. Using the GAIA simulation data, we analyzed neutral wind shear in the E region. We found that the wind shear is larger in the east Asian region the northern hemispheric summer, and in the South American region in the southern hemispheric summer, which is consistent with the previous observations. We will discuss the mechanism of dependence of the Es occurrence on geographical locations.

Keywords: sporadic E layer, atmosphere, ionosphere, model, neutral wind shear, occurrence

Introduction of long-term whole atmosphere-ionosphere simulation database and future update

JIN, Hidekatsu^{1*} ; MIYOSHI, Yasunobu² ; FUJIWARA, Hitoshi³ ; SHINAGAWA, Hiroyuki¹ ; MATSUO, Tomoko⁴

¹National Institute of Information and Communications Technology, ²Kyushu University, ³Seikei University, ⁴National Oceanic and Atmospheric Administration

The origins of upper atmospheric variations do not only come from the solar activities and rotation, but also from the Earth's lower atmosphere. In order to now-cast and forecast the upper atmospheric disturbances and variations, we have developed a whole atmosphere-ionosphere coupled model called GAIA. The model incorporates the Japanese meteorological reanalysis (JRA) into its lower atmospheric part as well as the daily F10.7 index, in order to reproduce the effects of realistic forcing both from the lower atmosphere and solar irradiance. We have carried out such simulation for the period from 1996 to 2014. The result shows that the model can reproduce major features of the observed ionosphere and thermosphere, including solar activity and rotation dependences, seasonal variations, shorter periodic variations, and effects of lower atmospheric disturbances such as stratospheric sudden warming [Jin et al., 2012; Liu et al., 2013, 2014]. We will show the comparison of the database and observations. We also introduce future update of the model, especially improvement of model accuracy using data assimilation technique.

Keywords: space weather, ionosphere, data assimilation, database, thermosphere, simulation

Beacon experiment of the ionosphere in Japan and southeast Asia

YAMAMOTO, Mamoru^{1*}

¹RISH, Kyoto University

We have been successfully conducted observations of total-electron content (TEC) of the ionosphere by the satellite-ground beacon experiment. An unique dual-band (150/400MHz) digital receiver GRBR (GNU Radio Beacon Receiver) were developed based on the recent digital signal processing technologies. The GRBR receivers were deployed first in Japan, and then in southeast Asia, and other areas. Data from the GRBR network were used for the investigations of variety of ionospheric phenomena. We have found mid-latitude summer nighttime anomaly (MSNA) over Japan, which is summer nighttime TEC enhancement at higher latitudes. Longitudinal "large-scale wave structures (LSWS)" in the low latitude were studied in detail as a source of equatorial Spread-F (ESF) events. Also we were successful to measure the equatorial ionospheric anomaly (EIA) near 100E longitude in large latitudinal extent of at most +/-20 degrees around the geomagnetic equator. The technique is utilized for sounding rocket-ground experiment as well. We review the ionospheric studies with the GRBR network, and will discuss future direction of the related studies.

Keywords: Satellite-ground beacon experiment, Total electron content, Middle- and low-latitude ionosphere, GRBR network

Statistical analyses on the thermal plasma density of the plasmasphere from the Akebono PWS observation

HASEGAWA, Shuhei¹ ; MIYOSHI, Yoshizumi^{1*} ; KITAMURA, Naritoshi¹ ; KEIKA, Kunihiro¹ ;
SHOJI, Masafumi¹ ; KUMAMOTO, Atsushi² ; MACHIDA, Shinobu¹

¹Solar-Terrestrial Environment Laboratory, Nagoya University, ²Department of Geophysics, Graduate School of Science, Tohoku University

The plasmasphere is a region of cold and dense plasma surrounding the Earth. The thermal plasma density of the plasmasphere is an important parameter for understanding the dynamics of the radiation belts as well as the inner magnetosphere, because the thermal plasma density controls the wave-dispersion relation, resonance conditions, etc. In this study, we conduct statistical analyses on the variations of the plasmasphere and plasmatrough, using electron density data derived from long-term plasma wave observations by the PWS experiments on board the Akebono satellite. We investigate the solar cycle variations of the thermal plasma density distribution. In deep plasmasphere, the thermal plasma density distributions along the field line do not significantly change during the solar cycle, and their distributions are well modeled as the diffusive equilibrium. On the other hand, the thermal plasma density distributions drastically change during the solar cycle in the outer portion of the plasmasphere. The thermal plasma density distributions are similar to the collisionless model during the solar active periods, while those are similar to the diffusive equilibrium model during the solar quiet periods. We also investigate time variations of the plasmaspheric density distribution during geomagnetic storms driven by CMEs and CIRs with superposed epoch analyses. The zero time corresponds to the minimum of the Dst index. The plasmaspheric density shrinkage depends on the storm amplitudes. The recovery time of the thermal plasma density is significantly different between CME- and CIR-storms. During the recovery phase of CIR-storms, the plasmapause does not recover quickly because of prolonged substorm activities during the high-speed streams. The recovery rates of the thermal plasma density depend on the L-shell, which is consistent with the previous studies. We find that the recovery rates of CME-storms are larger than that of CIR-storms.

Keywords: plasmasphere, electron density, akebono satellite, solar-cycle, geomagnetic storm

Solar Active Regions: From Birth to Eruption

TORIUMI, Shin^{1*}

¹National Astronomical Observatory of Japan

Solar-terrestrial environment is largely influenced by flares and CMEs sourced from the Sun. In particular, stronger events are known to be produced from solar active regions (ARs) including sunspots. Therefore, it is of great importance to understand the creation mechanism of ARs and their relationship with solar eruptions. Now it is widely accepted that ARs are caused by emerging magnetic flux, which is created by the dynamo effect in the convection zone. As a result of this flux emergence, several magnetic elements of the same polarity merge together at the solar surface and eventually form a single sunspot. Observations have revealed that large and complex ARs, the so-called delta sunspots, produce stronger flares. This may be because the free magnetic energy (or non-potentiality) is stored in such complex, sheared ARs with larger magnetic flux. Recent developments in the numerical modeling of flux emergence and flare eruptions open the door to further understanding of physical mechanisms behind such events. For example, our numerical simulations suggest that the flare-productive quadrupolar AR NOAA 11158, which is responsible for many X- and M-class flares, is produced from a single flux tube that is greatly disturbed in the convection zone during its emergence process. In this presentation, motivated by the above scientific curiosity, we review the observational and theoretical progress in the field of flux emergence, AR formation including delta-sunspots, and the resultant triggering of flare eruptions. After that, we discuss the future prospects.

Keywords: the Sun, active region, flux emergence, flare, MHD

Observational Study of the Flare Trigger Process

BAMBA, Yumi^{1*} ; KUSANO, Kanya¹

¹STEL/Nagoya Univ.

Solar Flares are explosive phenomena driven by magnetic energy stored in the solar corona. Because interplanetary disturbances associated with solar flares sometimes impact terrestrial environments and infrastructure, understanding the flare-triggering mechanism is important not only from a solar physics perspective but also for space weather forecasting. There are numerous observational studies and numerical simulations which attempted to reveal the onset mechanism of solar flares. However, because different observations support different models, the underlying mechanism of flare onset remains elusive, and the predictability of flare occurrence is limited.

To elucidate flare-trigger mechanism, Bamba et al. 2013 investigated four major flare events that occurred in active regions NOAA 10930 and NOAA 11158. We used data obtained by the Solar Optical Telescope (SOT) onboard the Hinode satellite. We analyzed the spatio-temporal correlation between the detailed magnetic field structure and the emission image of the Ca II H line at the central part of flaring regions for several hours prior to the onset of flares. We observed that characteristic magnetic disturbances developed at the centers of flaring regions in the pre-flare phase. These magnetic disturbances can be classified into two groups depending on the structure of their magnetic polarity inversion lines; to the so-called "Opposite-Polarity (OP)" and "Reversed-Shear (RS)" magnetic field recently proposed by Kusano et al. 2012. The result strongly suggests that some major flares are triggered by rather small magnetic disturbances. We also show that the critical size of the flare-trigger field varies among flare events and briefly discuss how the flare-trigger process depends on the evolution of active regions.

Because of the limitation of SOT field of view, however, only four events in the Hinode data sets have been utilizable in our previous study. Therefore, increasing the number of events is required for evaluating the flare trigger model. Bamba et al. 2014 investigated the applicability of data obtained by the Solar Dynamics Observatory (SDO) to increase the data sample for a statistical analysis of the flare trigger process. SDO regularly observes the full disk of the sun and all flares although its spatial resolution is lower than that of Hinode. We investigated the M6.6 flare which occurred on 13 February 2011 and compared the analyzed data of SDO with the results of Bamba et al. 2013 using Hinode/SOT data. Filter and vector magnetograms obtained by the Helioseismic and Magnetic Imager (HMI) and filtergrams from the Atmospheric Imaging Assembly (AIA) 1600Å were employed. From the comparison of small-scale magnetic configurations and chromospheric emission prior to the flare onset, we confirmed that the trigger region is detectable with the SDO data. We also measured the magnetic shear angles of the active region and the azimuth and strength of the flare-trigger field. The results were consistent with Bamba et al. 2014. We concluded that statistical studies of the flare trigger process are feasible with SDO as well as Hinode data.

X5.4/X1.3 flares on 7 March 2012: Exploring the energy storage, trigger and release of solar flares

SHIMIZU, Toshifumi^{1*} ; INOUE, Satoshi²

¹ISAS/JAXA, ²STE laboratory, Nagoya University

Solar flares abruptly release the free energy stored as a non-potential magnetic field in the corona and may be accompanied by eruptions of the coronal plasma. This presentation will focus on active region NOAA 11429, which appeared on the solar disk in March 2012. This active region produced X5.4 and X1.3 flares on 7 March 2012. They are a candidate of case studies examined by ISEST working group in the VarSITI project. The coronal mass ejection (CME) associated with them propagated in the interplanetary space and caused a large magnetic storm on the earth on 9 March. The active region contains delta-type sunspots, showing a strong shear in the entire system. One of important aspects relevant to space weather prediction is to understand physical processes of flare triggers. For a sheared magnetic field structure, the inclusion of a small-scale trigger field near the magnetic neutral line has been considered as one of key magnetic configurations leading to the occurrence of large flares. The Hinode Solar Optical Telescope provided a high accuracy measurement of vector magnetic field at the solar surface, allowing us to identify the trigger field on the neutral line responsible for the X5.4 flare. Moreover, the Doppler velocity measurements revealed that high-speed material flow exists in the horizontally oriented magnetic field formed nearly in parallel to the polarity inversion line and it existed at least from 6 hours before the onset of the flare, and that the high-speed material flow gradually develops the bipole structure, pushing the trigger field located at the destination of the flow and evolving the magnetic structure favorable for the onset of the eruptive flare. The observations suggest that gas dynamics at the solar surface play a vital role of leading to the onset of flares. The further observations show that another large flare (X1.3 flare) was triggered about one hour later at the west part of the neutral line, Why was the entire sheared magnetic structure not erupted at one time and were two steps taken for energy release? How does the gas dynamics on the solar surface contribute the trigger of the X1.3 flare? The non-linear force free field extrapolation from the observed vector magnetic field at the solar surface inferred the magnetic field configuration in the corona and the twistness of the magnetic field. The location of chromospheric flare ribbons as a function of time tells which twisted field is involved in the temporal evolution of the energy release. The talk will show the magnetic field configuration and dynamics of the active region and discuss the energy storage and trigger of the solar flares.

Keywords: Solar flare, Hinode, Photospheric magnetic field, corona, coronal field, space weather

Homologous flare occurred at the quadrupole field

KAWABATA, Yusuke^{1*} ; SHIMIZU, Toshifumi²

¹Department of Earth and Planetary Science, The University of Tokyo, ²Institute of Space and Astronautical Science, JAXA

Many models of the solar flare are suggested and they can explain some of the observed flares. However, they cannot explain all of the observed flares. The purpose of our study is investigating such events. We focus on homologous flares, which occur at the same location in the same active region repeatedly. We used Solar Optical Telescope (SOT) on board *Hinode* and Atmospheric Imaging Assembly (AIA) on board *Solar Dynamics Observatory (SDO)*. We can obtain three dimensional vector of the magnetic field by using the spectropolarimetric data of SOT and investigate the coronal configurations by using the extreme ultraviolet data of AIA. We analyze the active region NOAA 11967 which produced three M class flares on 2014 February 2. These flares show homology and the magnetic field at the flaring region is quadrupole. There were four flare ribbons and they showed rapid slipping motion. The photospheric flow can be seen between the sunspot and this flow may play a role in storing free energy and triggering the flare.

Keywords: solar flare, magnetic reconnection

Study on the Solar Flare Trigger Mechanism by using 3D Data Driven Magnetohydrodynamic Simulations

MUHAMAD, Johan^{1*} ; KUSANO, Kanya¹ ; INOUE, Satoshi¹

¹STEL, Nagoya University

Solar Flare can unleash large amount of energy from the Sun into the solar system and may affect global space based technologies on Earth. However, the detail process of the solar flare mechanism, especially in the early phase of the flare, is still not completely understood. It is believed that initially flare takes place from the highly sheared magnetic field in the active region of the Sun which contains very large non-potential energy. This strong sheared field is then destabilized by some trigger processes which responsible in releasing the free energy through some eruptions.

Several results from the previous numerical simulation study (Kusano et al., 2012) suggested that small magnetic flux which is imposed to the various simple magnetic structures can trigger the eruptions. Two different types of small magnetic structures near the polarity inversion line (PIL) are suggested as the possible configurations for the trigger of flares. They are the small bi-pole fields of opposite polarity or reversed shear compared to the highly sheared magnetic field in the scale of active region. Started from this result, we extend this work by using more realistic configuration of magnetic fields which mimic the solar coronal magnetic structure.

In this presentation, we will present some results of our simulations to elucidate the trigger process of solar eruption based on the 3D magnetohydrodynamic (MHD) model. In order to do this, we perform Nonlinear Force Free Field (NLFFF) extrapolation (Inoue et al., 2014) using the vector magnetogram data of the active region NOAA 10930 from the Hinode satellite. The NLFFF of the active region before the eruption showed that strong sheared magnetic field appeared near the PIL. We systematically carried out the numerical simulations, in which several emerging fluxes are injected onto different points in the NLFFF. As a result, we confirmed that some types of small emerging flux can trigger the eruption. It verifies that the previous work mechanism (Kusano et al. 2012) can be applied to more realistic magnetic structure. Our result suggests that the position and intensity of the emerging flux with respect to the initial NLFFF condition is very crucial for triggering the solar eruption.

References:

- [1] Magnetic Field Structures Triggering Solar Flares and Coronal Mass Ejections, K. Kusano, Y. Bamba, T. T. Yamamoto, Y. Iida, S. Toriumi, and A. Asai, 2012 ApJ 760 31 doi:10.1088/0004-637X/760/1/31
- [2] Nonlinear Force-Free Extrapolation of the Coronal Magnetic Field Based on the Magnetohydrodynamic Relaxation Method, Inoue, S., Magara, T., Pandey, V. S., Shiota, D., Kusano, K., Choe, G. S., Kim, K. S., 2014 ApJ 780 101 doi:10.1088/0004-637X/780/1/101

Keywords: Solar Flare, MHD Simulation, Nonlinear Force Free Field, Active Region

Properties of large amplitude geomagnetic sudden commencement (SC)

ARAKI, Tohru^{1*} ; SHINBORI, Atsuki²

¹Polar Research Institute of China, ²Research Institute for Sustainable Humanosphere, Kyoto University

Araki [2014; EPS] confirmed that SC occurred on March 24, 1940 was largest since 1868. The amplitude is 310nT at Alibag and more than 273nT at Kakioka. Using the experimental relationship between SC amplitude dH and dynamic pressure P_d associated with interplanetary shock (IPS) [Siscoe et al. ; 1968], $dH = A * d(P_d^{0.5})$, the corresponding P_d increase was estimated as 400-500nPa.

When the magnetosphere is compressed by IPS, field aligned currents (FACs) and ionospheric currents (ICs) are induced in addition to the primary magnetopause current (MPC). The LT variations of SC amplitude is produced by them which should be taken into account in estimation of P_d using Siscoes relationship.

When P_d is larger than about 30nPa, the magnetopause enters into the inside of the geosynchronous orbit. At that time the configuration of the MPC, FAC and IC might be different and contribute differently to the LT variation of SC amplitude. Thus it is important to examine the LT variation of large SCs and reflect the result in estimation of P_d associated with IPS.

Here we study properties of large amplitude SC including its LT variation. .

Keywords: geomagnetic sudden commencement(SC), interplanetary shock, LT variation, large amplitude

Progress in Understanding the Earth-affecting Coronal Mass Ejections

GOPALSWAMY, Nat^{1*}

¹NASA Goddard Space Flight Center

Coronal mass ejections (CMEs) producing solar energetic particle (SEP) events at Earth and causing geomagnetic storms are obviously the Earth-affecting CMEs. The occurrence of SEP events depends on the outer structure of CMEs, viz. the MHD shock, irrespective of the internal structure. On the other hand, geomagnetic storms occur when the internal magnetic structure of CMEs and/or the sheath behind the shock contain southward-pointing magnetic fields. The source locations of these two types of CMEs are also different: SEP events require magnetic connectivity to Earth, whereas storm-producing CMEs need to be directed toward Earth. Observations from the STEREO mission have contributed enormously to the study of Earth-affecting CMEs because of the expanded field of view and viewing angles away from the Sun-Earth line. The increased field of view closer to the Sun helped us understand that shocks can form as close as about 1.25 solar radii from the Sun center. The onset of type II radio bursts associated with CMEs has shown that shocks can form at large distances from the Sun (tens of solar radii). SEPs are energized as soon as the shock forms and can continue until the shock arrival at Earth and even afterwards. Therefore, predicting SEP events is generally very difficult (there is little lead time). There is definitely 1-4 days of lead time in predicting geomagnetic storms. There have been many attempts to predict the shock arrival using CME, Type II radio, and IPS observations. The CME trajectory can be severely affected by nearby coronal holes, non-radial ejection, and preceding CMEs resulting in large deviations in the predicted arrival times. We are far from predicting the orientation and strength of the CME magnetic field, which is crucial in predicting the occurrence and strength of geomagnetic storms. Then there are problems like the extremely mild space weather during solar cycle 24. Even though there are sufficiently large number of energetic CMEs ejected from the Sun, they do not seem to produce very many high-energy SEP events and large geomagnetic storms. It appears that this strange behavior can be attributed to a combination of weak solar activity and CME propagation in the altered heliosphere. This talk summarizes some of these issues related to Earth-affecting CMEs and how the issues will be tackled by the ISEST/MiniMax24 project of the SCOSTEP/VarSITI program.

Keywords: Coronal mass ejections, Solar Energetic Particle Events, Geomagnetic Storms, CME propagation, Solar Cycle, SCOSTEP/VarSITI

GEMSIS-Sun: Numerical Modeling of Sun-Earth System on the Basis of Solar Observations (SUSANOO)

SHIOTA, Daikou^{1*} ; KATAOKA, Ryuh² ; MIYOSHI, Yoshizumi¹ ; KUSANO, Kanya¹ ; YAMANOUCHI, Yuya¹

¹Solar-Terrestrial Environment Laboratory, Nagoya University, ²National Institute of Polar Research

Solar wind including coronal mass ejections (CMEs) is a main driver of various space weather disturbances. MHD modeling of the solar wind is a powerful tool to understand the solar-terrestrial environment and to forecast space weather accurately. Recently, we have developed an MHD model of the inner heliosphere on the basis of minimal input, namely, time series of daily synoptic observation of the photospheric magnetic field [Shiota et al. 2014]. The time series of MHD parameters at the Earth position is passed to a radiation belt model [Miyoshi et al. 2004] for forecasting of the radiation belt energetic electron flux. These programs are executed everyday on a server in STEL, Nagoya University and the results are uploaded on the web site (<http://st4a.stelab.nagoya-u.ac.jp/susanoo/>). This system is named as Space-weather-forecast-Usable System Anchored by Numerical Operations and Observations (SUSANOO). The calculated time profiles of solar wind velocity and magnetic field at positions of planets agreed with in situ measurements around solar minimum (2007 -2009) [Shiota et al. 2014].

The MHD simulation of solar wind does not include CMEs and therefore this is a possible source of error of the forecast in active period in solar cycle. We have been developing a CME model including magnetic flux ropes [Kataoka et al. 2009]. In the model, each CME is injected as a twisted magnetic flux rope accompanying with a velocity pulse through the inner boundary of the simulation and propagate into the solar winds. Thanks to the including flux ropes, the model is capable for a model of Dst index variation. We attempted to model the solar wind profile when multiple CMEs came from associated recent large-scale active regions: NOAA 10486 in October to November 2003 (Halloween event). As a result, the strength of compressed magnetic field becomes as high as about four times of background IMF when a fast CME interacts with the background solar wind. However, successive CMEs interact with each other to form much stronger magnetic field due to compression of the magnetic cloud of the preceding CME by shock associated the following CME.

Keywords: solar wind, MHD, radiation belt, space weather, CME

Quantitative Evaluation of Solar Wind Prediction Model "SUSANOO-SW" by Comparison with in-situ Measurements

YAMANOUCHI, Yuya^{1*} ; SHIOTA, Daikou¹ ; KUSANO, Kanya¹

¹Solar-Terrestrial Environment Laboratory, Nagoya University

The solar wind disturbance is one of the most important elements in the space weather. The space weather forecast is the attempt of predicting the disturbance before arrival at the earth. At present, in the most reliable prediction, we usually use in situ solar wind observations by space probes, locating in front of the earth, like the Advanced Composition Explorer (ACE). However, we can get the leading time about only 1 hour for which the solar wind propagates through the ACE-Earth distance because we cannot know the information of the solar wind before arrival at the ACE position by using only this method. Accordingly, magnetohydrodynamics (MHD) simulation enable to predict the further future solar wind.

In recent years, our group have developed a space weather prediction model: SUSANOO (Space-weather-forecast-Usable System Anchored by Numerical Operations and Observations), which can predict fluctuation of high-energy electrons in the radiation belt based on minimal input, real-time observation of the solar photospheric magnetic field. SUSANOO's solar wind model (SUSANOO-SW) [Shiota et al. (2014)] is the MHD simulation reproducing three-dimension structure of solar wind in the inner heliosphere with magnetic field model and empirical model for the solar surface magnetic field data. The calculated time profiles of solar wind velocity and interplanetary magnetic field (IMF) at positions of planets agreed with observed ones in solar minimum (2007 - 2009): the correlation coefficients of one-year time profiles of velocity and IMF ranges 0.54 - 0.73 and 0.40 - 0.58, respectively [Shiota et al. (2014)]. It can be interpreted that this model can reproduce well the global structure of the solar wind. However, when we focused on shorter time scale variation (period of one rotation), often see some disagreements. The cause of these disagreements can be included in the setting of the inner condition of SUSANOO-SW. Its improvement is needed for practical forecast.

In this research, we performed the SUSANOO-SW for a period from the solar minimum to the solar maximum (2007 - 2014). We evaluated the capability of the model by their comparison with in situ measurements in the following criteria: (1) the correlation coefficient of the velocity fluctuation for each Carrington Rotation (CR), (2) the percentage of agreement of velocity and magnetic field: (2-a) polarity of magnetic field, (2-b) velocity difference, (2-c) the sign of dv / dt . In the evaluation (2), we judged agreement by the hour and then we calculated the percentage of the agreement. As a result, the correlation coefficients are greater than 0.5 in CRs of 42.5%. The percentage of 'YES' for each criterion in evaluation (2) is larger than that of 'NO.' According to the results, we examined how the inner boundary condition on the timing of the disagreements with observation, and discuss possible improvement of the models for the inner boundary conditions.

Keywords: solar wind, space weather, MHD

Numerical Analysis of Instability of M-shape Flux Rope in the Solar Corona

ISHIGURO, Naoyuki^{1*} ; KUSANO, Kanya¹

¹Solar-Terrestrial Environment Laboratory, Nagoya University

The stability of magnetic flux rope in the solar corona is an important issue to understand the onset mechanism of solar flares and the formation of coronal mass ejections (CMEs). The instability of axisymmetric flux rope, called torus instability, is proposed to be the primary driver of solar eruption by Kliem and Toeroek (2006). They analyzed the ideal magnetohydrodynamic (MHD) stability of toroidal electric current channel for the mode of self-similar expansion, and concluded that the decay index of environmental magnetic field determines the criterion of the instability. However, several observations suggested that flux rope forms a non-axisymmetric loop in pre-eruptive state. In particular, the flux rope of M-shape structure, in which magnetic field line is concave above a magnetic polarity inversion line, is thought to be related to the onset of solar eruption. For instance, Moore et al. (2001) explained how the M-shape flux rope can be formed and erupts by tether-cutting reconnection. Recently, Kusano et al. (2012) found that the pre-flare reconnection between the sheared arcade and the small-scale magnetic flux of typical orientations favors the formation of M-shape flux rope and well triggers the tether-cutting reconnection scenario. However, the critical condition for the instability of the M-shape flux rope is still unclear.

In this paper, we numerically study the stability and dynamics of the M-shape flux rope. We model the M-shape flux rope using two current carrying tori which connect each other above the polarity inversion line and are anchored on the solar surface. The equilibrium condition is derived from the force balance of the hoop force of tori and the Lorentz force acting from external magnetic field. We also solve the equation of motion for the altitude of magnetic dip under the constraint that magnetic flux across the flux rope is conserved. As a result, the M-shape flux rope can be destabilized if the intensity of electric current exceeds the criterion and the altitude of magnetic dip ascends to the critical height. The numerical solution indicates that the decay index at the critical height of magnetic dip is substantially lower than the criterion of axisymmetric torus instability. It suggests that the M-shape flux rope much easily erupt than the theoretical prediction of axisymmetric torus instability, and the filament eruption may start even from a lower position where the decay index is lower than the conventional criterion.

Keywords: Sun, instability, flare, CME

Power-law relation between temperature and density in a prominence and a coronal cavity

KANEKO, Takafumi^{1*} ; YOKOYAMA, Takaaki¹

¹The University of Tokyo

In this study, we discuss the formation mechanism of a solar prominence by the radiative condensation by using MHD simulations including optically thin radiative cooling and thermal conduction. Our main focus is on the relationship between the temperature and density in a prominence and its coronal cavity.

Solar prominences are the cool dense plasma clouds in the hot tenuous corona. The formation model of prominences has not been established completely. The radiative condensation is believed to be a key process.

In the previous study, we proposed a model through the radiative condensation triggered by the formation of a flux rope: The flux rope is formed by the reconnection after imposing converging and shearing motion on the footpoints of the coronal arcade field. The radiative condensation is triggered by the thermal nonequilibrium inside the flux rope. We have demonstrated this model in our simulations and found an empirical scaling law between the temperature and the density of a prominence.

The remained issues in our previous study were that the prominence in our simulations had much higher temperature than that of the observed one, and that the physical meaning of the scaling law was unclear due to the unrealistic small contrast of temperature and density between the prominence and the corona.

In this study, we allow the prominence temperature in our simulations to be lower, and reproduce more realistic prominences. As a result, we successfully extend the previous empirical scaling law to a power law both in a prominence and its surrounding coronal cavity. We also found that the power depends on the temperature gradient of each field line.

Keywords: solar prominence, solar filament

Properties of sub-arcsecond transition-region structures at the footpoints of coronal loops in the active-region plage

KIMURA, Yasuhisa^{1*} ; HARA, Hirohisa²

¹University of Tokyo, ²National Astronomical Observatory of Japan

The energy release above the photosphere of 5,800 K produces the chromosphere of ten thousand degrees and the corona of a million degrees. The building block of the corona is a coronal loop that connects two magnetic polarities with opposite signs on the photosphere. The width of coronal loops that are observed with the most X-ray and EUV telescopes is broader than an arcsecond in angular distance, which is limited by the angular resolution of the telescopes. Coronal loops are considered to have sub-structures with a narrower width, threads, within the observed structures, as inferred from the measured volume filling factor and multiple Doppler-shift components at the footpoint of a coronal loop, both of which were found by the Hinode EUV observations. The HiC sounding-rocket EUV imaging observations with 0.3'' spatial resolution have recently shown the direct evidence for such small-scale structures in coronal loops. Observations of the sub-arcsec coronal structures will be of crucial importance in understanding the mechanism of coronal heating. We do not, however, have high-resolution coronal imaging data outside the HiC observing period of five minutes. In order to access the sub-arcsecond structures in the coronal loops, we have analyzed the data from Atmospheric Imaging Assembly (AIA) and Interface Region Imaging Spectrograph (IRIS). While AIA observes the coronal structures in 1.2 arcsec resolution with 12 sec cadence, IRIS mostly observes the chromosphere and transition region in 0.4 arcsec with 10 sec cadence, latter of which is the region located between the chromosphere and corona. Our idea is to use IRIS imaging observations in a Si IV emission line for studying the sub-arcsecond coronal threads that connect to the transition-region structures at the coronal base in the active-region plage where the unipolar vertical kG magnetic fields are found at the photosphere. We have found intermittent structures in a Si IV line with 0.5-1.0 arcsec FWHM diameter in intensity at the base of the coronal loops. The intensity and position of such sub-arcsec structures in Si IV change with time within a cross section of a coronal loop at the base. In addition, the intensity of coronal loops at the base increase with a time lag of 10-30 sec after the appearance of the sub-arcsec TR structures in Si IV line. We will discuss what structures are formed in broader coronal loops and the formation mechanism.

Keywords: sun, coronal loop, transition region, IRIS

On Physical condition in the early Heliosphere

SUZUKI, Takeru^{1*}

¹School of Science, Nagoya University

In this talk, I would like to discuss the evolution of physical properties in the heliosphere at early epochs. After briefly reviewing the evolution of the protoplanetary disk with particularly focus on the role of turbulence-driven disk wind, I introduce the evolution of the solar wind. We also discuss effects of variation of the physical condition in the heliosphere on the formation and evolution of solar-system planets.

Keywords: Solar Wind, Protoplanetary Disk, Magnetohydrodynamics, wave, turbulence

Shock formation of Alfvén waves in a non-uniform medium

SHODA, Munehito^{1*}; YOKOYAMA, Takaaki¹

¹Department of Earth and Planetary Science, University of Tokyo

Alfvén waves, generated by photospheric granule motion, are considered to play a significant role in the energetics of coronal heating and solar wind acceleration. In many theoretical Alfvén wave models, coronal high temperature is supported by continuous energy supply by Alfvén waves and the ponderomotive force due to the local dissipation of Alfvén waves is responsible for solar wind acceleration. In linear theory dissipation due to viscosity and diffusivity is the only way to take out wave energy, which is too inefficient for coronal heating. Therefore some nonlinear processes such as phase mixing, shock formation and turbulent heating are the promising mechanisms for coronal heating and solar wind accelerations.

In this study we concentrate on shock heating among some nonlinear processes. The aim of our research is to estimate the shock formation time of Alfvén waves in a non-uniform medium. In case of uniform media, shock formation time is estimated analytically, while in non-uniform case it is not yet investigated sufficiently. We perform one-dimensional magnetohydrodynamic simulations for the estimation of shock formation time. A rightward-going Alfvénic wave packet of single wavelength is set initially and we calculate its nonlinear propagation. Background magnetic field is assumed to be uniform and only the density is set to be non-uniform in our simulation. The shock formation time is obtained by Fourier spectrum evolution. Due to the non-uniformity of the background, nonlinearity of Alfvén waves decreases as they propagate, which leads to the retardation and prevention of shock formation. We compare our numerical results with weakly nonlinear analytical results and show its validity. Analytical results, expressed by Lambert's W function, indicates that in the corona Alfvén waves hardly steepen, whereas in the interplanetary space the background condition is favorable for shock formation.

Keywords: Alfvén wave, coronal heating, solar wind

Propagation and reflection of nonlinear Alfvén wave in the solar chromosphere

KONO, Shunya^{1*} ; YOKOYAMA, Takaaki¹

¹The University of Tokyo

It has been suggested that Alfvén waves, generated in the photosphere and propagating along the magnetic flux tube, can carry enough energy to the low-plasma-beta region in the upper chromosphere and the dissipation of waves is one of the possible mechanisms to heat the solar chromosphere. Temperature of the chromosphere is low and the plasma gas is partially ionized. The collisions between plasmas and neutrals cause additional diffusion of the magnetic fields, which is called ambipolar diffusion. On the other hand, the compressible waves are generated by the nonlinear effect of the magnetic pressure associated with the Alfvén waves propagating upwards from the photosphere, and form shock waves in the chromosphere. In previous studies, it has been indicated that the dissipation of generated shock waves can give enough thermal energy to heat the chromosphere. The effect of the magnetic diffusion to the nonlinear propagation of Alfvén waves in the chromosphere has not been investigated enough. Some observations show the reflection of Alfvén waves at the top boundary of the chromosphere, which is called the transition region. It is important to discuss the dissipation mechanisms of waves in consideration of the reflection mechanism at the top and bottom boundaries of the chromosphere.

In this study, we investigate the reflection of Alfvén waves propagating along a vertically open magnetic flux tube in the chromosphere at the transition region and photosphere. If we assume the atmospheric condition in the solar quiet region, the damping length of waves which have frequencies of 1–100 mHz by the magnetic diffusion is estimated to become much larger than the thickness of the chromosphere. For investigating the dissipation of Alfvén waves in the chromosphere, we should consider the condition where the reflection at the photosphere and transition region efficiently occurs and more Alfvén waves are trapped in the chromosphere. We investigate the propagations of the nonlinear Alfvén waves by performing one-dimensional numerical simulations. As a result, 60–70 % of the incident Alfvénic pulse waves with frequencies of 10–100 mHz are reflected at the transition region. Most of reflected waves from the transition region penetrate into the convection zone without being reflected at the bottom of the photosphere. We perform simulations in different magnetic field structures and confirm that the results are almost the same in any cases. It is considered to be important to take the energy flux going from the top and bottom boundaries of the chromosphere into account for the dissipation of Alfvén waves in the chromosphere. In the case where the initial velocity amplitude of Alfvén wave is set to be 1.0 km s^{-1} , the compressible waves generated by the nonlinear effect may have enough energy to heat the chromosphere. If the initial velocity amplitude is set to be smaller, less compressible waves are generated and other dissipation mechanisms of the Alfvén waves may become effective.

Keywords: chromospheric heating, Alfvén wave, magnetic diffusion, nonlinear

Characteristics that enhance white-light emission in solar flares

WATANABE, Kyoko^{1*} ; MASUDA, Satoshi² ; KITAGAWA, Jun²

¹Institute of Space and Astronautical Science, Japan Aerospace Exploration Agency, ²Solar-Terrestrial Environment Laboratory, Nagoya University

In association with large (such as X-class) solar flares, we sometimes observe enhancements of visible continuum radiation, which is known as a "white-light flare". Because many white-light events show a close correlation between the time profiles and locations of white-light emission, and the hard X-rays and/or radio emission, it is believed that the origin of white-light emission is non-thermal electrons. However, not all large solar flares have white-light enhancements, and non-thermal electrons exist even in micro-flares. There should be some necessary condition to generate white-light enhancements.

To understand what conditions generate a white-light flare, we analyzed 42 M- and X-class flares observed with Hinode/SOT during the period from January 2011 to August 2013. Comparing the white-light (19 events) and no white-light (23 events) events, we concluded that the key factor needed to generate white-light enhancement is the precipitation of large amounts of nonthermal electrons into a compact region within a short time duration (Kitagawa et al., submitted to ApJ).

In this paper, we present the statistical results until December 2014. Not only the Hinode/SOT white-light (G-band (4305A) and continuum (Blue: 4505A, Green: 5550A, Red: 6684A)) data, but we also check SDO/HMI continuum data. The total number of events is now about twice that of Kitagawa's study. We compared the white-light emission data with GOES, hard X-ray emission data and/or the strength of the photospheric magnetic fields and looked for any relationship between them.

Keywords: solar flare, white-light, particle acceleration

Characteristics in solar white-light flares based on radio observations

MASUDA, Satoshi^{1*} ; KITAGAWA, Jun¹ ; WATANABE, Kyoko²

¹Solar-Terrestrial Environment Laboratory, Nagoya University, ²Institute of Space and Astronautical Science, Japan Aerospace Exploration Agency

White-light flare is a solar flare in which an enhancement in white-light continuum is detected. Although most of white-light flares are large flares in energy like GOES X-class flare, it is not correct that only the amount of released energy determine if a solar flare becomes a white-light flare. To understand what generates a white-light flare, we analyzed 42 M- and X-class flares observed with Hinode/SOT during the period from January 2011 to August 2013. Among these 42 events, the number of white-light flares was 19. Comparing the white-light and no white-light events, we concluded that the key factor to generate white-light enhancement is the precipitation of large amount of nonthermal electrons within a short time duration into a compact region (Kitagawa et al., submitted to ApJ).

In this paper, we analyzed the 10 events (white-light: 4 events, no white-light: 6 events) among the 42 events, which were observed with Nobeyama Radio Heliograph (NoRH) and Nobeyama Radio Polarimeters (NoRP). GHz microwave are emitted by gyrosynchrotron from very-high energy (\sim MeV) accelerated electrons. The peak intensity in 17 and 35 GHz does not show any significant difference between the white-light and no white-light events. This indicates that such high-energy electrons does not contribute white-light enhancement. The spectrum of gyrosynchrotron emission usually has a peak frequency which corresponds to the turning point (turn-over frequency) between the optical thick part in the lower frequency range and the optically thin part in higher frequency range. The white-light flares show systematically high turn-over frequency than that of the no white-light events. The higher turn-over frequency might correspond to stronger magnetic field. This is consistent that white-light flares tend to be compact. As for the time evolution of the spectrum, the no white-light flares tend to show the spectral hardening. This indicates that the magnetic mirror effectively works in no white-light flares because of the weak magnetic field in the flare loop.

Keywords: solar flare, particle acceleration

Two-dimensional simulation of the small scale structure in the solar chromosphere

IJIMA, Haruhisa^{1*} ; YOKOYAMA, Takaaki¹

¹Department of Earth and Planetary Science, Graduate School of Science, The University of Tokyo

Recent observation revealed the highly dynamic and fine structures in the solar chromosphere. The solar chromosphere is known to have wide range of the plasma beta, high nonlinearity with shock waves, cooling from the radiation, thermal conduction by the non-thermal electron, and weak ionization rate. All of the processes above have opportunity contributing to the dynamics of the solar chromosphere. In order to get the proper interpretation of the observation in the solar chromosphere, the numerical simulation with the various effects can be very useful tool. In our study, a new radiative magnetohydrodynamic code is developed for the dynamical simulation of the solar chromosphere. The numerical domain includes the upper part of the convection zone to the lower part of the corona. The convective motion as a driver of the dynamics in the upper atmosphere is consistently modeled using the radiative transfer calculation and the realistic equation of state. The thermal conduction from the non-thermal electron is also included. In this talk, we will report the numerical implementation from this numerical code and the first results filled with small scale structures in the two-dimensional domain.

Keywords: solar chromosphere, wave, convection, magnetohydrodynamics

Millimetric observation of the solar chromosphere and space weather using the Nobeyama 45m radio telescope

IWAI, Kazumasa^{1*} ; SHIMOJO, Masumi¹

¹Nobeyama Solar Radio Observatory, National Astronomical Observatory

The atmospheric structure of the solar chromosphere is basic information to understand the heating mechanisms of the solar atmosphere and various solar phenomena. Hence, the investigation of the chromosphere is also important for the space weather. The main emission mechanism of the Sun in millimeter and submillimeter wavelength range is a thermal free-free emission from the chromosphere. This emission is formed under local thermodynamic equilibrium (LTE) conditions. The opacity of the thermal free-free emission is determined by the electron temperature and density. In addition, the Rayleigh-Jeans law can be applied in this wavelength range. Hence, the observed brightness temperature at several frequency bands can be converted into the thermal electron temperature of the radio source region. However, large millimeter and submillimeter telescopes usually cannot observe the Sun because they are not designed to observe such a high-brightness body. Hence, there have been only a few high-resolution solar observations at this wavelength range. In this paper, we report on the first single-dish observation of the chromosphere at 85 and 115 GHz with sufficient spatial resolution for resolving the sunspot umbra using the Nobeyama 45 m telescope. We used radio attenuation material, i.e. a solar filter, to prevent the saturation of the receivers. We found that the brightness temperature distribution at millimeter range strongly corresponds to the ultraviolet (UV) continuum emission at 1700 Å, at both active and quiet regions. The upper limit of the brightness temperature of the sunspot umbra is almost the same as that of the quiet region. However, the plage region exhibits a higher brightness temperature than the quiet Sun. The 45 m telescope has broad side-lobes, and the sunspot region is surrounded by a brighter plage region. Hence, the actual brightness temperature of the umbra region should be lower than the observational result. This result is inconsistent with the preexisting chromospheric models, which predict that the sunspot umbra should be brighter than the quiet region at millimeter range. This result suggests that an actual height of the transition region can be lower than that of the pre-existing models.

Keywords: Sun, Radio radiation, millimeter, Chromosphere, space weather

Wide energy electron precipitation associated with the pulsating aurora and its impact on the middle atmosphere

MIYOSHI, Yoshizumi^{1*} ; OYAMA, Shin-ichiro¹ ; SAITO, Shinji¹ ; KURITA, Satoshi¹ ; FUJIWARA, Hitoshi² ; KATAOKA, Ryuho³ ; EBIHARA, Yusuke⁴ ; KLETZING, Craig⁵ ; REEVES, Geoff⁶ ; SANTOLIK, Ondrej⁷ ; CLILVERD, Mark⁸ ; RODGER, Craig⁹ ; TURUNEN, Esa¹⁰ ; TSUCHIYA, Fuminori¹¹

¹Solar-Terrestrial Environment Laboratory, Nagoya University, ²Seikei University, ³National Institute of Polar Research, ⁴RISH, Kyoto University, ⁵University of Iowa, USA, ⁶Los Alamos National Laboratory, USA, ⁷Charles University in Prague, Czech Rep., ⁸British Antarctic Survey, UK, ⁹University of Otago, NZ, ¹⁰Sodankyla Geophysical Observatory, University of Oulu, Finland, ¹¹PPARC, Tohoku University

The pulsating aurora are caused by intermittent precipitations of tens keV electrons. It is also expected that not only tens keV electrons but also sub-relativistic/relativistic electrons precipitate simultaneously into the ionosphere owing to whistler-mode wave-particle interactions. We analyzed the pulsating aurora event in November 2012 using several ground-based observation data; EISCAT, riometer, and sub-ionospheric radio waves, and the Van Allen Probes satellite data. The electron density profile obtained from EISCA Tromso VHF radar identify the electron density enhancement at >68 km altitudes. The electron energy spectrum derived from the inversion method indicates the wide energy electron precipitations from 10 keV ? 200 keV. The riometer and network of subionospheric radio wave observations also showed the energetic electron precipitations during this period. During this period, the footprint of the Van Allen Probe-A satellite was very close to Tromso and the satellite observed rising tone emissions of the lower-band chorus (LBC) waves near the equatorial plane. Using the satellite observed LBC and trapped electrons as an initial condition, we conducted a computer simulation of the wave-particle interactions. The simulation showed simultaneous precipitation of electrons at both tens of keV and a few hundred keV, which is consistent with the energy spectrum estimated by the inversion method using the EISCAT observations. This result revealed that electrons with a wide energy range simultaneously precipitate into the ionosphere in association with the pulsating aurora. We also discuss the possible impacts on the middle atmosphere due to precipitations of wide energy electrons during the pulsating aurora.

Keywords: energetic electron precipitation, Geospace, middle atmosphere

Radiation dose of aircrews during solar proton events

KATAOKA, Ryuho^{1*} ; SATO, Tatsuhiko²

¹National Institute of Polar Research, ²Japan Atomic Energy Agency

A significant enhancement of radiation doses is expected for aircrews during ground-level enhancement (GLE) events, while the possible radiation hazard remains an open question during non-GLE solar energetic particle (SEP) events. Using a new air-shower simulation driven by the proton flux data obtained from GOES satellites, we show the possibility of significant enhancement of the effective dose rate of up to 4.5 uSv/h at a conventional flight altitude of 12 km during the largest SEP event that did not cause a GLE. As a result, a new GOES-driven model is proposed to give an estimate of the contribution from the isotropic component of the radiation dose in the stratosphere during non-GLE SEP events. We show further development of our radiation dose model with some applications, including the most recent GLE 72 occurred on 16 Jan 2014.

Keywords: solar proton events, radiation dose

Variation of trace chemical species induced by solar energetic particles in the middle atmosphere: ozone and nitric acid

NAKAI, Yoichi^{1*} ; MOTIZUKI, Yuko¹ ; MARUYAMA, Manami¹ ; AKIYOSHI, Hideharu² ; IMAMURA, Takashi²

¹RIKEN Nishina Center, ²National Institute for Environmental Studies

Influences on the terrestrial environment of super solar flares have attracted interests recently. In a super solar flare, a large amount of protons, X-rays, gamma-rays etc. emitted from the surface of the sun intrude into the terrestrial atmosphere, which is called a solar energetic particle (SEP) event. In particular, high-energy protons come down to the stratosphere. The SEP protons can induce dissociation of nitrogen molecules. A part of dissociated nitrogen atoms contribute to increase of odd nitrogen oxides (NO_x) and reactive odd nitrogen species (NO_y). Consequently, the SEPs influence the ozone concentration through the chemical reactions in the atmosphere.

We have performed simulations for variation of chemical composition in SEP events by solving a large number of rate equations for concentrations of chemical species without taking into account of transport processes, i.e., simple Box-model simulations. More than 70 chemical species including ions and about 480 chemical reactions are adopted in the present simulation. A large number of ionic processes including recombination in the stratosphere were treated for the first time to our knowledge.

We assume that the energy deposits from the SEP protons to the chemical species determine the yields of prompt products. As a result, we can consider the prompt products to be generated from nitrogen and oxygen molecules of major components of the air. The estimation of the energy deposit is carried out using the calculations of ion-pair creation by the SEP protons [1]. For the yield estimation of the prompt products, the G-values are used [2,3], where the G-values are given by amount of products per absorbed energy of 100eV. During a SEP event, we deal with both the photochemical reactions and the reactions induced by the SEP protons in the simulation. Variation of chemical composition in a SEP event is estimated as a difference between the result of the simulation including the processes triggered by the SEP protons and that by taking account of only photochemical reactions.

In this talk, we will mainly report the results by our Box-model simulation for the variations of ozone and nitric acid for the SEP event observed in October-November 2003.

References

- [1] C.H. Jackman et al., *Atmos. Chem. Phys.* **8**, 765 (2008).
- [2] C. Willis and A. W. Boyd, *Int. J. Radiat. Phys. Chem.* **8**, 71 (1976).
- [3] H. Mätzing, *Adv. Chem. Phys.* **LXXX**, 315 (1991).

The solar modulation of galactic cosmic rays during the cycle 23/24

MIYAKE, Shoko^{1*} ; YANAGITA, Shohei²

¹National Institute of Technology, Ibaraki College, ²Ibaraki University, Faculty of Science

The intensity of galactic cosmic rays depends on the strength of the interplanetary magnetic field (IMF), the polarity of the IMF, tilt angle of the current sheet, and the velocity of the solar wind. So we have to take into account these parameters in the numerical simulation of the solar modulation of galactic cosmic rays.

In this presentation, we present the results of the numerical simulation of the solar modulation of galactic cosmic rays during the cycle 23/24. We also discuss about the solar modulation during the cycle 25.

Keywords: galactic cosmic ray, solar modulation, heliosphere, Interplanetary magnetic field

Variation of the intensity of galactic cosmic rays during the Maunder Minimum

MIYAHARA, Hiroko^{1*} ; HORIUCHI, Kazuho² ; TOKANAI, Fuyuki³ ; KATO, Kazuhiro³ ; MORIYA, Toru³ ;
YOKOYAMA, Yusuke⁴ ; MATSUZAKI, Hiroyuki⁴ ; MOTOYAMA, Hideaki⁵ ; KATAOKA, Ryuho⁵

¹Musashino Art Univ., ²Hirosaki Univ., ³Yamagata Univ., ⁴The Univ. of Tokyo, ⁵NIPR

Variations of the galactic cosmic-ray flux during the Maunder Minimum (AD1645-1715) are examined based on carbon-14 in tree rings and beryllium-10 in ice cores. Variations of beryllium-10 content in ice cores have suggested that the flux of galactic cosmic rays have increased by ~40 percent for about one year around every other solar cycle minima, when solar dipole magnetic field was negative. Periodicity of the events is ~26-28 years, corresponding to the Hale cycle during the Maunder Minimum. These extreme enhancements of cosmic rays are suggested to be possibly caused by a change in the large scale structure of heliospheric magnetic field, associated with extremely weakened solar activity. To obtain more reliable ages for those events, we have been also measuring the carbon-14 content in tree rings dated by dendro-chronology.

Keywords: Maunder Minimum, cosmic rays, solar activity, heliosphere, space climate, cosmogenic nuclide

Open Data of Sunspot and aurora records in the Chinese chronicles : 7th to 13th century

HAYAKAWA, Hisashi² ; TAMAZAWA, Harufumi^{1*} ; KAWAMURA, Akito D.¹ ; ISOBE, Hiroaki³

¹Kwasan and Hida Observatories, Graduate School of Science, Kyoto University, ²Graduate School of Advanced Integrated Studies in Human Survivability, Kyoto University, ³Kyoto University Unit of Synergetic Studies for Space

Records of sunspots and aurora observations in pre-telescopic historical documents can provide useful information about solar activity in the past. This is also true for extreme space weather events, as they may have been recorded as large sunspots observed by the naked eye or as low-latitude auroras. In this study, we present the results of a comprehensive survey of sunspots and aurora records in Chinese formal chronicles spanning the 7th to 13th . This chronicles contain records of continuous observations with well-formatted reports conducted as a policy of the government. A brief comparison of the frequency of sunspots and aurora observations and the observations of radioisotopes as an indicator of the solar activity during corresponding periods is provided. In our project, we survey and compile the sunspots and aurora records in historical documents from various locations and languages, ultimately providing it to the academic community, not only community of natural science but also human and social sciences, as open data.

Keywords: sunspot, aurora, archaeoastronomy, extrem space weather

Why big sunspot 12192 did not produce CME ?

SHIBATA, Kazunari^{1*} ; ISHII, Takako¹ ; KAWAMURA, Akito¹

¹Kwasan and Hida Observatories, Kyoto University

The sunspot 12192 had an area 2750 MSH (Millionth Solar Hemisphere), which was the biggest in recent 24 years after the appearance of the sunspot 6368 (3080 MSH) in November 1990. Hence this sunspot attracted many people's interest, and had been suspected to produce big flares and big magnetic storms. In fact, this spot produced 6 X-class flares during two weeks between 17 Oct and 30 Oct. This was the most number of X-class flares per one active region during this cycle. However, curiously, these 6 X-class flares did not lead to coronal mass ejections (CME), so that the solar wind in these weeks had been quiet and there were no major magnetic storms. The Hida Observatory of Kyoto University succeeded to observe two X-class flares (X1.1 flare at UT0503 (peak time) of 19 Oct and X3.1 flare at UT2140 (peak time) of 24 Oct) that occurred in this region, using SMART telescope and Domeless Solar Telescope (DST).

In this talk, we will report the detailed observations of the big sunspot 12192 as well as X-class flares in this region, and discuss why this big sunspot did not produce CME even though it produced 6 X-class flares, giving the conclusion that the bigger the sunspot area, the more difficult to produce CME for the flares with the same X-ray intensity.

Keywords: flare, CME, sunspot, magnetic field, magnetohydrodynamics, space weather prediction

Investigation of surface magnetic flux transport by use of Hinode/SOT and SDO/HMI

IIDA, Yusuke^{1*} ; HOTTA, Hideyuki²

¹Japan Aerospace Exploration Agency, ²High Altitude Observatory

Since magnetic field on the solar surface triggers various solar activities, it is very important to understand their structure in terms of the space weather. An important issue is transport mechanism of magnetic flux. It is thought that the flow dominates the magnetic field on the solar surface. Although the transport is treated as a pure diffusion process for long time, recent solar observations suggest the differences from the diffusion.

We reported the relationship between the travel distance of the magnetic flux concentration and the elapsed time from the birth of the concentrations. The sub-diffusion scaling was found in the time range longer than 2×10^4 seconds for the first time. The investigation is, however, limited because the analysis is done by using the magnetogram obtained by Solar Optical Telescope onboard the Hinode satellite (Hinode/SOT), which does NOT cover the whole Sun. Thus in this study we investigate the relationship with the Helioseismic and Magnetic Imager on board the Solar Dynamics Observatory (SDO/HMI), which covers the whole Sun. Since the spatial resolution of SDO/HMI is lower than that of Hinode/SOT, we use both telescopes in order to see the influence of the resolution on the analysis. We find the similar sub-diffusion scaling with the power law index of 0.7 ± 0.1 . SDO/HMI shows a slightly larger magnitude. This difference may come from the difference of spatial resolution between the telescopes. In the presentation, we also plan to show the 3D MHD simulation of the magneto-convection if time permits.

Keywords: Sun, convection, magnetic field, diffusion

Solar cycle phase and occurrence of intense space weather events

WATARI, Shinichi^{1*} ; WATANABE, Takashi¹

¹National Institute of Information and Communications Technology

Length and shape of solar cycle expressed by sunspot number change cycle to cycle. We need to normalize this to discuss on dependence of solar cycle phase of intense space weather events. For example, it is important to study whether intense space weather events occur uniformly in a solar cycle or not. We normalize shape of cycles using length, rise time, and fall time of cycles. In our presentation, we will report our result of analysis on large flares, intense geomagnetic storms, and so on.

Keywords: solar cycle, space weather, extreme event

Electric field and currents in the ionosphere-ground circuit during space weather disturbances

KIKUCHI, Takashi^{1*} ; HASHIMOTO, Kumiko² ; EBIHARA, Yusuke³ ; TOMIZAWA, Ichiro⁴ ; WATARI, Shinichi⁵

¹Nagoya University/Solar-Terrestrial Environment Laboratory, ²Kibi International University, ³Kyoto University, Research Institute for Sustainable Humanosphere, ⁴Center for Space Science and Radio Engineering, Univ. of Electro-Communications, ⁵National Institute of Information and Communications Technology

When the CME or CIR hit the magnetosphere, the electric field and currents are generated by the dynamos in the magnetosphere and transmitted to the polar ionosphere down the magnetic field lines and further to the low latitude ionosphere. The transmitted electric field drives the Hall currents that close with themselves in the high-midlatitude ionosphere and the field-aligned currents close with the Pedersen currents that extend to the equatorial ionosphere near-instantaneously, where the Pedersen currents are intensified considerably by the Cowling effect appearing as the equatorial electrojet (EEJ). Thus, the geomagnetic disturbances often appear concurrently at high latitudes and the dayside equator with magnitude decreasing with latitude but amplified at the equator. At midlatitudes, the electric fields transmitted from high latitude are detected with the HF Doppler sounder, which are well correlated with the EEJ. The concurrent development of the midlatitude electric field and EEJ is commonly observed during the storm sudden commencements (SC), geomagnetic PC and Pi pulsations, quasi-periodic DP2 and storm/substorm convection and overshielding events. As shown in this paper, disturbances in the GIC (geomagnetically induced currents) on the ground are also well correlated with the EEJ and electric field in the ionosphere. The observations suggest that the electric current flows from the dynamo in the magnetosphere into the ground via the ionosphere. The ionospheric currents and GIC are connected by the displacement currents flowing on the wave front of the TM₀ (TEM) mode waves propagating in the Earth-ionosphere waveguide (ionosphere-ground transmission line) [Kikuchi, 2014], where the Poynting flux is transported in the neutral atmosphere between the ionosphere and ground.

Responses of polar cap ionosphere to successive CMEs in Dec 2014: 5 days continuous monitoring with two all-sky imagers

HOSOKAWA, Keisuke^{1*} ; TAGUCHI, Satoshi² ; SHIOKAWA, Kazuo³ ; OGAWA, Yasunobu⁴ ; OTSUKA, Yuichi³

¹University of Electro-Communications, ²Graduate School of Science, Kyoto University, ³Solar-Terrestrial Environment Laboratory, Nagoya University, ⁴National Institute of Polar Research

In December 2014, three coronal mass ejections (CMEs) occurred successively during 4 days interval from December 18 to 21. These CMEs arrived at the Earth respectively at December 21, 22 and 23 and caused a small magnetic storm (Dst \sim -50 nT). During this interval, two all-sky airglow imagers were operative in Longyearbyen, Norway (78.1N, 15.5E) and Resolute Bay, Canada (74.7N, 265.1E) and monitoring the polar cap ionosphere continuously for 5 days from December 20 to 24. The two all-sky imagers observed continuous generation/propagation of polar cap patches from the dayside towards the nightside across the polar cap region during a prolonged interval of southward IMF Bz. Such a continuous transportation of high-density plasma is visualized for the first time. At the time of the arrival of second CME, the IMF Bz was directed strongly northward. During this period, the polar cap shrank significantly, which implies that the magnetosphere was almost closed during such a strongly northward IMF condition. By using the 5 days continuous optical data in the polar cap region, we will discuss various responses of polar cap ionosphere to CME-induced solar wind disturbances.

Keywords: Polar cap, Polar cap patches, Polar cap aurora, Coronal Mass Ejection (CME)

Laboratory experiment with heavy ion beam for verification of new particle formation by cosmic rays

SUZUKI, Asami^{1*} ; MASUDA, Kimiaki¹ ; ITOW, Yoshitaka¹ ; SAKO, Takashi¹ ; MATSUMI, Yutaka¹ ;
NAKAYAMA, Tomoki¹ ; UEDA, Sayako¹ ; MIURA, Kazuhiko² ; KUSANO, Kanya¹

¹Solar-Terrestrial Environment Laboratory,Nagoya University, ²Tokyo university of science

It is considered that the solar activity may affect the global climate, but the correlation mechanism is still not understood. One of the possible mechanisms for the correlation is the cloud formation by the galactic cosmic rays, which are modulated by the variation of solar magnetic activity. This relation was clearly indicated by the good correlation observed for the galactic cosmic-ray intensity and the global low-cloud amount. This hypothesis includes the ion-induced nucleation model, in which new particles in the atmosphere are created efficiently through atmospheric ions produced by cosmic rays, and finally these particles grow up to the size of cloud condensation nuclei. In this study, a laboratory experiment for verification of the hypothesis has been conducted with a reaction chamber. A flow of clean air with water vapor, ozone and sulfuric dioxide was introduced to a metallic chamber, where we irradiated UV light for solar irradiance and beta rays or accelerator beam for cosmic rays. The beam of the heavy ion accelerator HIMAC at National Institute of Radiological Sciences was used in the present experiment.

The result so far showed that ion density in the chamber increased due to the heavy ion irradiation and enhancement of the number of aerosol particles due to its was confirmed. In this presentation, I will report the results of the heavy ion irradiation experiments. Heavy ion beam of nitrogen and xenon was used because their ionization loss is different by a factor of 60. The ionization loss could be an index representing the ability to ionize the air molecules that is, parameters that contribute to atmospheric ion generation. Since it is considered that the aerosol particle generation would be increased according to the amount of ions, the experiment was carried out for these ions. The results showed that produced ion density was not different for both ions with different ionization power, and aerosol particle production efficiency was almost the same. The less ionization density for Xe ions might be due to large recombination of produced ions along the ion beam tracks.

Global cooling and mass extinction driven by a dark cloud encounter

NIMURA, Tokuhiko^{1*} ; EBISUZAKI, Toshikazu² ; MARUYAMA, Shigenori³

¹Okayama Astronomical Museum, ²RIKEN, ³Earth-Life Science Institute, Tokyo Institute of Technology

We found a broad positive anomaly in iridium across over ~ 5 m in a pelagic deep sea sediment core sample, in addition to a spike in iridium at the K-Pg boundary related to the Chicxulub asteroid impact. Any mixtures of materials on the surface of the Earth cannot explain the broad iridium component. On the other hand, we found that an encounter of the solar system with a giant molecular cloud can explain the component, if the molecular cloud has a size of ~ 100 pc and the central density of ~ 2000 protons/cc.

Kataoka *et al.* (2013; 2014) pointed that the encounter with a dark cloud may drive an environmental catastrophe to lead a mass extinction. The solid particles from the dark cloud accreted onto the Earth and stayed for several months or years in the stratosphere: Since their sunshield effect is as large as -9.3 W m^{-2} , it can be a cause of a global climate cooling in the last 8 Myr of Cretaceous period, which is suggested by the variations of stable isotope ratios in oxygen (Barrera & Savin, 1999; Li & Keller, 1999; 1998; Barrera & Huber, 1990) and strontium (Barrera & Savin, 1999; Ingram, 1995; Sugarman *et al.*, 1995). The resultant extensions of the continental ice sheet cause a regression of the sea level, too. The global cooling seems to be associated with the decrease in the diversity of fossils, which eventually lead to the mass extinction at the K-Pg boundary.

The mass extinction at K-Pg boundary is widely thought to be caused by an impact of an asteroid (Alvarez *et al.*, 1980; Schulte *et al.*, 2010) at 65.5 Ma. However, a complete extinction of the total family by just one asteroid impact seems rather difficult because of the following two reasons. (1) A severe environment turn-over would finish few years after impact, the solid particles and sulphate launched by the asteroid impact is settled down for only few months (troposphere) to few years (stratosphere) and negative radiative forcing become negligible after a few years from the impact. (2) There were similar impacts without environmental catastrophe on the Earth, for example, Woodleigh, Chesapeake and Popigai craters. However, there are no evidences of association for mass extinction. It is difficult to explain why only Chicxulub impact leads mass extinction but the other three comparable impacts did not.

It is worth noting that the encounter with the dark cloud can perturb the orbit of asteroids and comets by its gravitational potential may cause asteroid impact or comet shower. The asteroid impact at K-Pg, therefore, may be one of the consequences of the dark cloud encounter.

We conclude that the cause of the climate cooling at the End-Cretaceous was driven by an encounter with a giant molecular cloud, with such an encounter and related perturbation in global climate a more plausible explanation for the mass extinction than a single impact event, Chicxulub.

Keywords: Nebula Winter, dark cloud encounter, Space Climate, End-Cretaceous, K-Pg boundary, mass extinction

Prediction Study of Solar Flare Events in GOES X-ray Flux using Time-Series Prediction Engine UFCORIN

MURANUSHI, Takayuki^{1*} ; SHIBAYAMA, Takuya² ; HADA MURANUSHI, Yuko³ ; ISOBE, Hiroaki⁴ ; NEMOTO, Shigeru⁵ ; KOMAZAKI, Kenji⁵ ; SHIBATA, Kazunari³

¹RIKEN Advanced Institute for Computational Science, ²Solar-Terrestrial Environment Laboratory, Nagoya University, ³Kwasan and Hida Observatories, Kyoto University, ⁴Unit of Synergetic Studies for Space, ⁵BroadBand Tower, Inc.

We have been developing UFCORIN, an automated space weather prediction system based on machine-learning technologies. Our aim is twofold: one is to provide real-time space weather forecast that thoroughly utilize the huge amount of solar observation data available today. The other is to discover the observational flare-triggering features, by analyzing the big data with the clear goal of predicting the solar flares.

UFCORIN stands for Universal Forecast Constructor by Optimized Regression of INputs. As the name suggests, UFCORIN is designed as a generic time-series predictor, which can be set to predict arbitrary time series from arbitrary numbers and kinds of input time series.

Using our system we predict maximum of GOES X-ray flux for 24-hour period in the future. As inputs to the predictor, we use wavelet powers of the full disk line-of-sight magnetogram obtained by the Helioseismic and Magnetic Imager (HMI) on board the Solar Dynamic Observatory (SDO). We also use the total magnetic flux data by SDO/HMI, and past data of GOES X-ray flux as inputs. The simulated prediction ran for 2 years (2011-2012) with 1-hour time resolution. To predict X, \geq M and \geq C class flares events, we first predict the real value of the GOES X-ray flux maximum, and then apply different thresholds for different events. These thresholds are part of the prediction parameter subject to optimization.

Following Bloomfield et al. [2012], we use true skill statistics (TSS) to compare the performance of various prediction strategies. Our best TSS values using HMI and GOES data are 0.692, 0.470 and 0.566, respectively, for predicting X, \geq M and \geq C class flares. These TSS values are comparable to previous studies such as those by Song et al. [2009], by Bloomfield et al. [2012], and by Bobra & Couvidat [2014]. We emphasize that we predict flares for the 2-years continuous period, and make no use of active region detection. In contrast, all of the previous studies are based on active region images and selected set of events.

At the annual meeting, we would also like to report the progress of our ongoing research, for example the search of flare features in SDO/AIA ultraviolet images. Also, our techniques can be applied to the prediction of space weather events other than solar flares, such as solar wind, solar energetic particles, and geomagnetic disturbances. We are also trying to quantify the social and economic impacts of the solar flares, in order to provide customized space weather forecast for various human activities.

Keywords: Solar flares, Space weather, Flare prediction, SDO, Big data, Machine learning

Prediction of foF2 variation above Tokyo using solar wind input to a neural network

UCHIDA, Herbert Akihito^{1*} ; MIYAKE, Wataru² ; NAKAMURA, Maho³

¹Graduate School of Engineering, Tokai University, ²Tokai University, ³Tokyo Gakugei University

Neural network has the ability to learn the empirical relation from input data. It is often used to produce empirical prediction models of several space environmental parameters. One operational model (Nakamura, 2008) used K-index input to predict foF2 variations and ionosphere storms above Tokyo. There are also several works for predicting geomagnetic indices such as Dst from the solar wind inputs (e.g., Watanabe et al., 2002). These studies lead us to expect that the prediction of foF2 at the disturbed situation can be more accurate when solar wind parameters are used to the inputs. Recently the availability of solar wind parameters from the Advanced Composition Explorer became longer enough to overlap one solar activity. In this study, solar wind proton velocity and IMF-By, IMF-Bz are used to the input to predict the foF2 disturbances above Tokyo. The K-index input model (Nakamura, 2008) was also recreated using the same data term as the SW input model. The SW input model tends to predict more often the negative disturbance cases, and it predicted daytime quick variations more accurate than the K-index input model. Statistical comparison of the predicting ability of those 2 models will be discussed, and the contribution of the solar wind input parameters to the foF2 will be tested using an artificial input.

Keywords: ionosphere, foF2, prediction, neural network, solar wind

Prediction of MeV electron flux throughout the outer radiation belt by multivariate autoregressive model

SAKAGUCHI, Kaori^{1*} ; NAGATSUMA, Tsutomu¹ ; SPENCE, Harlan² ; REEVES, Geoffrey³

¹National Institute of Information and Communications Technology, ²University of New Hampshire, ³Los Alamos National Laboratory

The radiation belts are consisted of relativistic energy electrons in MeV range. The electron flux in the outer belt is highly variable depending on both solar wind and magnetospheric conditions. Enhanced fluxes sometimes cause deep dielectric charging on spacecraft and therefore satellite anomaly happens after the discharge. Prediction of such MeV electron variations is needed for safety operation of the satellite in the near Earth's orbit, but the physical processes of acceleration, loss, and transport of relativistic electrons are not fully understood so far. Japanese space weather information center at NICT has developed a multivariate autoregressive (AR) model for the prediction of electron flux at geostationary orbit (GEO). The model can estimates future flux variations by a few days lagging response of solar wind parameter changes [Sakaguchi et al., 2013]. Now, we have developed new models to predict electron flux variation throughout the outer radiation belt at L=3-6. Observation data of 2.3 MeV electrons in 2012-2014 by Van Allen Probes are used as predictor time series variate. The appropriate combinations of explanation variate are examined and selected respectively for each of L value ($\Delta L=0.2$) model among geomagnetic indices (AE, Kp, Dst) as well as solar wind parameters (speed, BZ, BS, Pdyn). The combinations of these variates systematically change according to L-value shift. In the presentation, we show the estimation method of multivariate AR coefficient matrixes and discuss about estimated combinations of explanation variate. Also we show past prediction results that were validated by observation data based on two skill scores of prediction efficiency and persistence.

Keywords: radiation belt, prediction, Van Allen Probes

Initial Observations of Space Environment Data Acquisition Monitor (SEDA) on Board Himawari-8

NAGATSUMA, Tsutomu^{1*} ; SAKAGUCHI, Kaori¹ ; KUBO, Yuki¹

¹National Institute of Information and Communications Technology

New Japanese meteorological satellite, Himawari-8, was successfully launched on October 7, 2014. Space environment data acquisition monitor (SEDA) is on board Himawari-8, as one of the housekeeping information for satellite operation. SEDA consists two sensors. One is proton sensor, which has 8 separate diode detectors. The energy range of the proton detectors are from 21.6 MeV to 81.4 MeV.

The other is electron sensor, which measures internal charging currents caused by energetic electrons. There are eight sensor plates arranged in a stack and each plate responds to a different energy range. As a result, energetic electrons whose energy range between 0.2 to 4.5 MeV can be measured by the electron sensors. The time resolution of each sensors is 10 sec. The field of view of SEDA is eastward. Thus, the specification of SEDA is suitable for monitoring the energetic electrons and protons above Japanese meridian of Geostationary orbit.

Himawari-8/SEDA has been operating since November 3, 2014. Based on the agreement between Japanese Meteorological Agency (JMA) and NICT, JMA is providing Himawari/SEDA data in near-real time since January 21, 2015. Currently we are checking the quality of Himawari-8/SEDA data. Results of initial observation by Himawari-8/SEDA will be introduced in our presentation.

Keywords: Space Weather Forecast, Geospace, Radiation Belts, Proton Event, High Energy Particles, Geostationary Orbit

Influence of solar wind on surface temperatures and climate teleconnection patterns

ITOH, Kiminori^{1*}

¹Yokohama National University

Correlation maps (spatial distribution of correlation coefficient) for various combinations between surface temperature (Ts) and the aa index (a measure of solar wind strength) as well as climate teleconnection patterns. Stratification based on the QBO (quasi-biennial oscillation at equatorial stratosphere) and sunspot number (SSN) was carried out. Time windows employed were from 10 years (shortest) to 73 years (longest).

Figure 1 shows examples where correlation between January aa and February Ts was examined for the period of 1942-2014. Each condition gave a correlation map with characteristic features. For instance, the map for easterly QBO and large SSN resembles that for the Arctic Oscillation (AO), and that for westerly QBO and middle SSN is similar to that for the Pacific Decadal Oscillation (PDO).

From these observations, we conclude that the influence of the solar wind on the climate is similar to that of teleconnection patterns in magnitude. The close relation between the solar wind and the AO is known well, but relation with other teleconnection patterns was found to be strong as well. The solar wind appears to excite various teleconnection patterns directly or indirectly.

Keywords: solar wind, aa index, teleconnection pattern, surface temperature, QBO

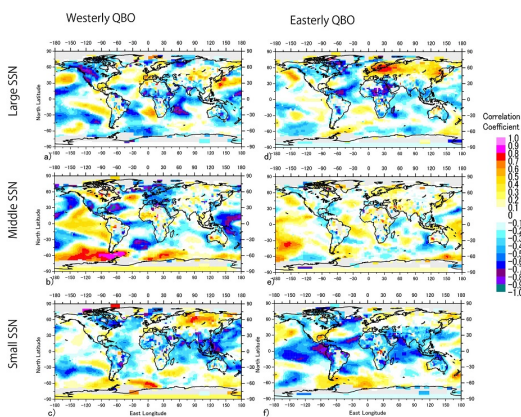


Fig. 1. Correlation maps for the aa index (January) vs. surface temperature (February) for 1942-2014, stratified using QBO phases (westerly or easterly) and sunspot number (Large, Middle, Small).